

## Cyclogenesis in Cold Air Masses

STEVEN BUSINGER

*Department of Marine, Earth and Atmospheric Sciences, North Carolina State University, Raleigh, North Carolina*

RICHARD J. REED

*Department of Atmospheric Sciences, University of Washington, Seattle, Washington*

(Manuscript received 15 May 1988, in final form 19 December 1988)

### ABSTRACT

The small-scale and rapid development of polar lows over relatively data-sparse areas results in a special forecast challenge for the operational forecasting community. This paper constitutes a review of recent advances in our understanding of cyclogenesis in polar air masses. The review is primarily comprised of a survey of the observed features of polar lows as documented in a number of case studies presented in the recent literature. The review is organized on the basis of a combination of observational and physical considerations and is aimed at diagnosing common types of developments. Theoretical ideas concerning the origins of polar lows and results of numerical modeling experiments aimed at simulating their development are also summarized. Finally, a discussion of approaches to the operational problem of forecasting polar lows is given.

### 1. Introduction

Operational weather forecasters have long been aware of the forecast problems associated with subsynoptic-scale cyclogenesis in the cold air masses over open water. These disturbances require special attention from the forecaster for several reasons. They often evolve quickly and can result in adverse weather conditions that affect the safety of operations at sea. Due to the violent and unforeseen nature of polar lows, Norwegian and Icelandic history is filled with tragic accounts of accidents involving small fishing boats. The scale of the disturbances is often too small for numerical weather prediction models to provide adequate forecast guidance. Until recently, weather forecasters were forced to rely on sparse observations from ships and islands to identify the position, motion and intensity of polar lows. While the introduction of satellite imagery has aided weather forecasters, it has also revealed an unexpected profusion of cyclonic disturbances in polar air masses behind or poleward of the polar front (World Meteorological Organization 1973; Anderson et al. 1969). The purpose of this paper is to provide a review of recent advances in our understanding of cold-air cyclogenesis in a framework that the authors hope will prove useful to the forecaster in dealing with this ubiquitous phenomenon.

The term "polar low" or "polar trough" was originally used by British meteorologists to describe cold air depressions that affect the British Isles (Meteorological Office 1962). Since some controversy surrounds, or at least in the past has surrounded, the use of the term "polar low", it is important to define at the outset what the authors mean by the term. We will use it here in a broad sense to denote any type of small synoptic- or subsynoptic-scale cyclone that forms in a cold air mass poleward of major jet streams or frontal zones and whose main cloud mass is largely of convective origin. We use the term "polar low" in a generic sense to include all phenomena that fit the above description. Some justification for this usage is provided by reexamination of cases that have gone under the rubric of polar lows in the early literature. Only by employing a broad definition of the term "polar low" can these varied cases be grouped together. A further discussion of the classification of polar lows is deferred to section 2.

In view of the paucity of observational data available to early investigators it is only recently that polar lows have become a focus of research (Harley 1960; Pedgley 1968; Lyall 1972; Harrold and Browning 1969; Mansfield 1974; Rasmussen 1977, 1979; Reed 1979). The lack of observations has contributed to the difficulty of synthesizing coherent physical models describing the triggering mechanisms and internal energetics of polar lows, and the slow progress that operational forecast models have made in predicting their development and movement.

---

*Corresponding author address:* Dr. Steven Businger, Department of Marine, Earth and Atmospheric Sciences, North Carolina State University, Raleigh, NC 27695-8208.

In recent years significant research efforts have been directed toward improving our knowledge of polar lows. Through a combination of field experiments [Arctic Cyclone Experiment (ACE) in February of 1984 (Shapiro and Fedor 1986); the Alaska Storms Experiment in February and March of 1985] and mesoscale modeling work [Seaman (1983); Sardie and Warner (1985); and Grønås, Foss and Lystad (1986a,b)], progress has been made in our understanding of these potentially destructive storms (Kellogg and Twitchell 1986; Rasmussen and Lystad 1987).

The framework for the overview of polar lows presented in this paper is derived from an observational as well as a physical perspective. In section 2, general characteristics of the systems and the larger environment in which they form are described. Three types of polar lows are distinguished: (i) short-wave/jet-streak type, (ii) Arctic-front type, and (iii) cold-low type. Discussions of case studies that are most representative each of the three types are presented in sections 3, 4 and 5, respectively. Multitype cases that represent combinations of the above types are discussed in section 6. Theoretical and numerical modeling studies relevant to polar lows are briefly summarized in section 7. A discussion that focuses on the problem of forecasting polar lows is presented in section 8. Finally, summary and conclusions are given in section 9.

## 2. General characteristics of polar lows

Polar lows span a continuum of scales, from a few hundred kilometers to more than 1000 km in diameter, and a wide range of intensities, from moderate breezes to hurricane force winds (Reed 1979; Locatelli et al. 1982; Rasmussen 1981, 1983; Mayengon 1984; Forbes and Lottes 1985; Shapiro et al. 1987).

Under favorable conditions, polar lows can intensify rapidly (e.g., Seaman et al. 1981; Rasmussen 1985; Shapiro et al. 1987; Rabbe 1987), producing strong surface winds and local heavy precipitation. Occasionally, they spawn severe thunderstorms. For example, seven tornados were reported in one storm that struck the California coast on 8 November 1982 (Reed and Blier 1986b). Heavy snowfalls over Britain and the Netherlands have also been attributed to polar lows (Harrold and Browning 1969; Seaman et al. 1981). Locatelli et al. (1982) noted that a significant number of the cyclones that affect the Pacific Northwest are polar lows, while Monteverdi (1976) found that as much as 50% of the annual precipitation in San Francisco is produced by nonfrontal disturbances occurring in the polar air mass and related only to positive vorticity advection (PVA) aloft.

Polar lows occur most often over the oceans in winter, originating in regions of enhanced convection and developing a comma- or spiral-shaped cloud pattern as they mature. The comma cloud shape is the result of the superposition of a positive vorticity center and

a moderate background current. If the magnitude of the background flow is small, the vorticity will produce a spiral cloud pattern (Fig. 1). (The polar low seen in Fig. 1 will be the subject of a forthcoming paper by the authors.) As an illustration of the seasonal variation of polar lows, the number of systems affecting the Norwegian coast or ships near the coast are shown in Fig. 2a. The maximum frequency occurs in the period between October and April. A 9 yr climatology of polar low occurrence in the Bering Sea and Gulf of Alaska (Fig. 2b) reveals a similar seasonal dependence and an even sharper winter peak.

The airstreams within which polar lows form are invariably characterized by cyclonic flow or shear (Reed 1979; Mullen 1979) by near neutral or unstable lapse rates in the boundary layer with conditionally unstable lapse rates extending locally as high as the middle to upper troposphere (e.g., Rasmussen 1977; Mullen 1979; Businger 1987) and by substantial heat and moisture fluxes from the underlying ocean (e.g., Reed and Blier 1986b; Shapiro et al. 1987). Composite charts (Fig. 3) of surface pressure and 1000–500-mb thickness for 42 cases of polar lows, reproduced from Businger (1985), clearly show that large cold pools of cyclonically rotating air provide the most favorable environment for polar-low outbreaks in the Norwegian and Barents seas. Similar results were found for polar-low outbreaks in the northern Pacific Ocean region (Businger 1987).

### a. Types of polar-low development

Some controversy continues as to whether there are several distinct types of polar lows with different underlying physical instability mechanisms, or whether these disturbances are basically varied manifestations of the same underlying physical mechanisms. The comma-shaped cloud system generally occurs in proximity to a trailing front or the jet stream axis and the spiral-shaped system tends to be located farther back in the polar or Arctic air mass (Locatelli et al. 1982). Rasmussen (1983) in a review article on mesoscale disturbances in cold air masses refers to the former type as “comma clouds” and the latter as “true” or “real” polar lows (sometimes also referred to as the “Arctic instability lows”). Locatelli et al. refer to both types as “vortices in polar air streams.”

As yet, no widely accepted method exists for classifying polar lows, although schemes have been proposed based on their appearance in satellite imagery (Carleton 1985; Forbes and Lottes 1985) and on the synoptic situation [Lystad, Hoem and Rabbe (in Lystad 1986); Rasmussen and Lystad 1987; Reed 1987]. To facilitate the organization of this review, we will differentiate three elementary types of polar-low development based on associated distinctive synoptic patterns. These types are also physically distinct in the degree and distribution of baroclinicity, static stability,

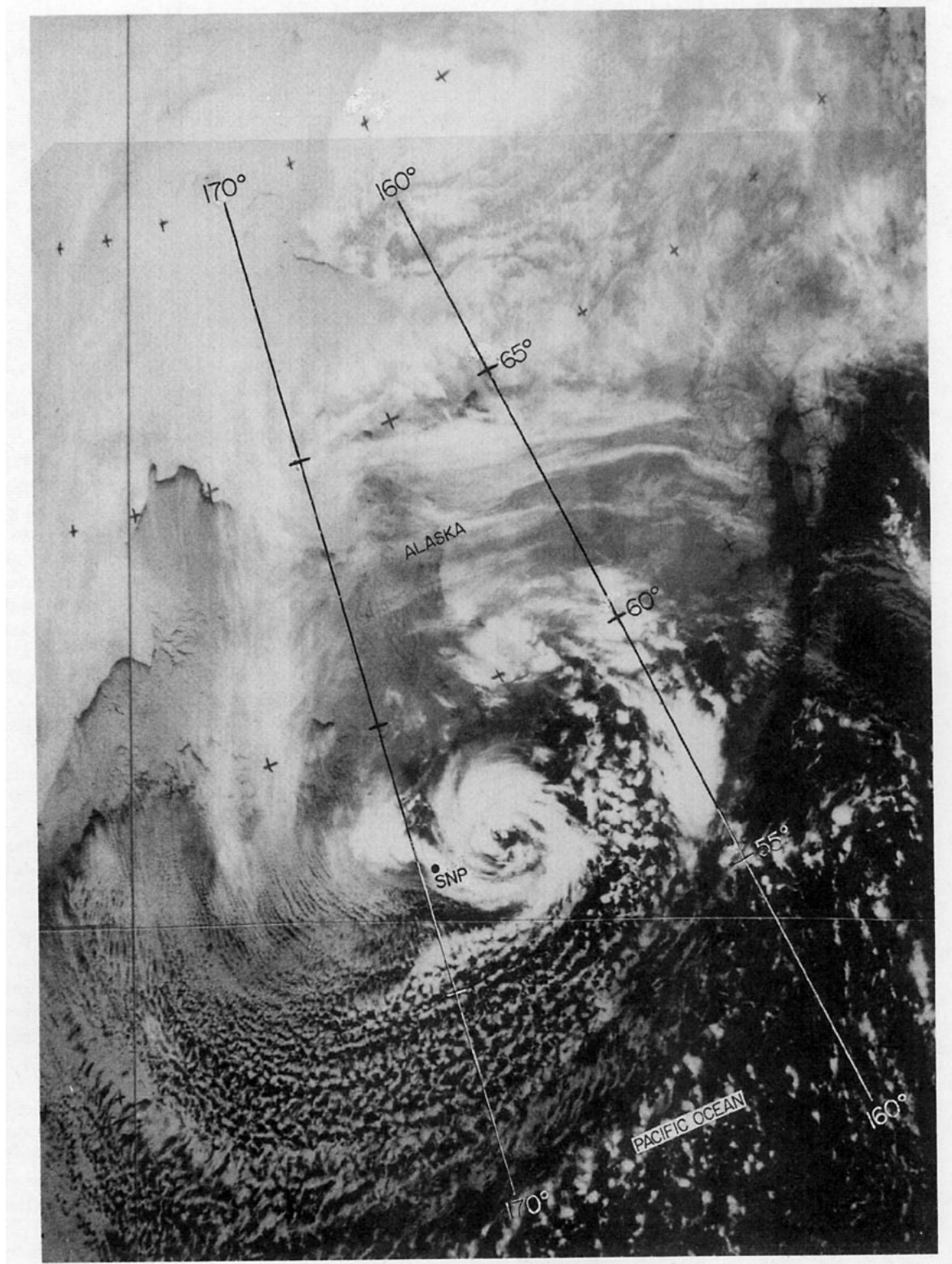


FIG. 1. A NOAA-5 infrared satellite photograph of a polar low and cloud streets over the Bering Sea at 2100 UTC 8 March 1977. SNP indicates the location of the rawinsonde station at St. Paul Island (R. Anderson, personal communication).

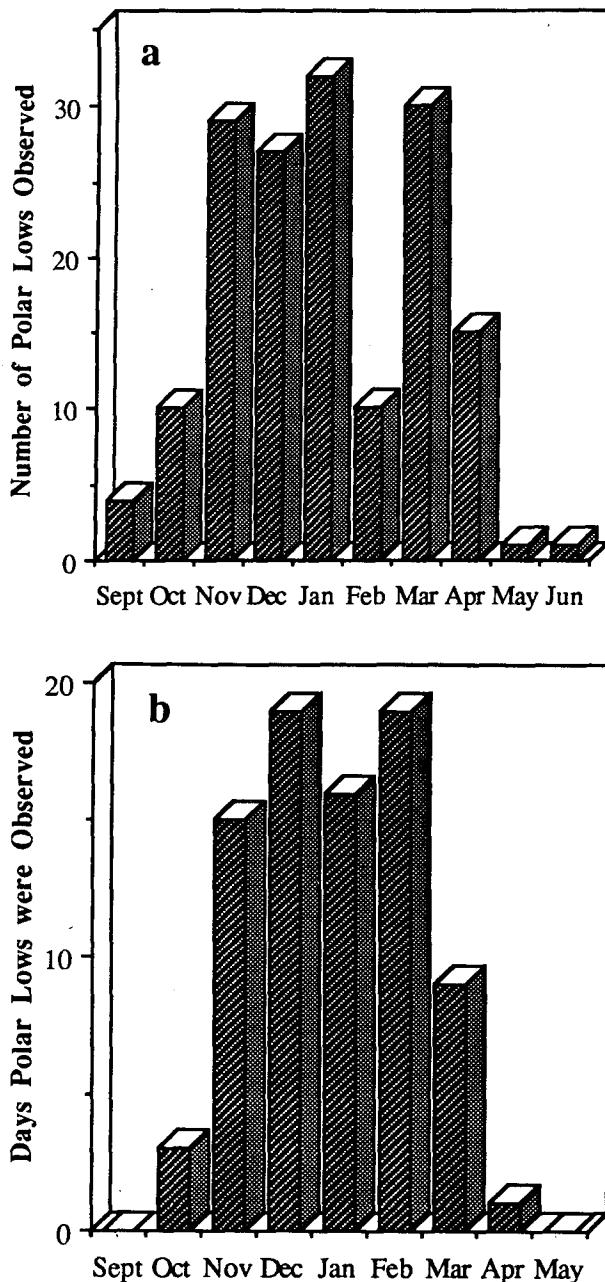


FIG. 2. (a) Frequency distribution of polar lows near Norway for the period 1971-85 (adapted from Lystad 1986) and (b) frequency distribution in the Bering Sea and Gulf of Alaska for the period 1975-83 (from Businger 1987).

and surface fluxes of latent and sensible heat. The three types are (i) short-wave/jet-streak type, characterized by a secondary vorticity maximum and PVA aloft, deep, moderate baroclinicity, and modest surface fluxes; (ii) Arctic-front type, associated with ice boundaries and characterized by shallow baroclinicity, and strong surface fluxes; and (iii) cold-low type, characterized by weak baroclinicity, strong surface fluxes, and deep convection. Of course it is possible for a com-

bination of the above types to exist. In some cases extreme winds ( $30-35 \text{ m s}^{-1}$ ) are associated with small, hurricane-like vortices embedded within a larger polar low or synoptic-scale low. It is not clear at this stage whether such systems should be regarded as a distinct class of polar low or as embedded substructure within a larger system. In any case they are of sufficient importance to warrant separate discussion in section 6.

### 3. Short-wave/jet-streak type

At the larger end of the spectrum of polar lows is the comma cloud. This type of polar low is characterized by a large mesoscale to small synoptic-scale, comma-shaped cloud pattern that develops in regions of enhanced tropospheric baroclinicity, often just poleward of preexisting frontal boundaries. The term "comma cloud" ascribed to this type of polar low is an abbreviation of "comma-shaped cloud pattern," and was introduced by satellite meteorologists to denote a characteristic cloud signature seen in cold air masses (Anderson et al. 1969; World Meteorological Organization 1973). Care must be exercised when using the term "comma cloud," however, since comma-shaped cloud systems occur on many scales, and the same terminology has been used to describe the cloud pattern accompanying midlatitude frontal cyclones (Carlson 1980; Carr and Millard 1985).

Examples of comma clouds can be found in Reed (1979), Mullen (1983), Reed and Blier (1986a,b), and Businger and Walter (1988). Figure 4 shows a satellite image of a well-developed comma cloud of small scale located to the rear of a synoptic-scale frontal cyclone.

Comma clouds form in regions of enhanced positive-vorticity advection (PVA) at midtropospheric levels (Anderson et al. 1969; Reed 1979). Typically the comma cloud starts as a region of enhanced convection in the PVA region ahead of an upper-level short-wave trough [or from an alternative point of view in the left front exit region of a jet streak (Uccellini and Kocin 1987)]. A surface trough (often marked TROF by United States analysts) lies near the rear of the comma tail. In the more strongly developed cases a low-pressure center lies beneath the comma head and the trough may assume frontal characteristics in the later stages of development (Locatelli et al. 1982; Mullen 1983; Reed and Blier 1986a,b). Weak to moderate baroclinicity exists within the cold air mass throughout the depth of the troposphere (Mullen 1979). A schematic representation appears in Fig. 5a. Using geostationary imagery, Zick (1983) showed that in some instances comma clouds over the Atlantic Ocean form from preexisting vorticity centers that migrate from the front to the rear side of large-scale troughs. The schematic in Fig. 5b depicts the evolution of the cloud shield associated with a developing comma cloud as the latter moves down the trailing side of a 500-mb trough.

Comma clouds can occur anywhere in the extratropical Pacific or Atlantic Oceans, but based on the

authors' experience, are most likely to form in the western oceans where the prevailing winds often transport cold, continental air across warm oceans currents. Convection develops in the cold air masses in response to heating and moistening of the boundary layer. Inspection of satellite imagery reveals that comma clouds typically form in regions of enhanced convection (Fig. 6), and that the convection becomes organized into banded structures as the comma clouds mature. Recent aircraft observations taken in a region of enhanced convection (shown in Fig. 6) over the Gulf of Alaska (Businger and Walter 1988), show that when the mean-wind profile is dominated by cold advection and the air is conditionally unstable through most of the troposphere, the rainbands tend to orient with their long axes parallel to the wind-shear vector and do not propagate with respect to the mean flow. Analysis of observations taken in comma clouds as they crossed the Washington coast (Businger and Hobbs 1987) shows that when the disturbances are dissipating and the mean-wind profile is dominated by warm advection, rainbands are found to be oriented perpendicular to the wind shear and propagate relative to the mean flow. A schematic depiction of a rainband in a comma cloud for this latter case is given in Fig. 7. For a discussion of physical mechanisms for the maintenance of rainbands in comma clouds the reader is referred to Parsons and Hobbs (1983), Businger and Hobbs (1987) or Businger and Walter (1988).

#### *a. Interactions between comma clouds and the polar front*

When a comma cloud and its accompanying region of PVA approach a polar front, a wave often develops on the front. In reviewing the literature on such interaction, it is evident that a variety of interactions occur (Anderson et al. 1969; Reed 1979; Carleton 1985). In cases where the separation is large, the wave may remain independent of the comma cloud and develop into a typical midlatitude cyclone. In cases of closer proximity, the comma cloud often merges with the frontal wave in a process termed "instant occlusion," in which frontogenesis associated with the comma cloud provides the occluded front and the frontal wave provides the warm and cold fronts to the storm (Anderson et al. 1969). After the instant occlusion these storms appear identical to classical occluded systems in the cloud signatures seen on satellite imagery.

Since comma clouds generally occur over oceans, few case studies of their interaction with polar fronts have been studied with the benefit of mesoscale observational data. Mesoscale analysis by Locatelli et al. (1982) of three comma clouds that affected the Washington coast showed that the advection and precipitation patterns associated with these comma clouds and polar fronts remained independent, even though they appeared to merge when viewing standard operational

data. Browning and Hill (1985) used a mesoscale dataset over the North Atlantic Ocean and Great Britain to describe the circulation pattern in a case where a polar trough interacted with a polar front. The authors developed a simple conceptual model that relates the principle cloud features to ascending air flows or conveyor belts. McGinnigle et al. (1988) analyzed several cases of instant occlusions over the North Atlantic Ocean using synoptic and mesoscale data and numerical model diagnostics. They suggest an alternative analysis scheme to the traditional instant occlusion in which the instant occlusion is replaced by a warm front, and the secondary cold front associated with the polar trough, becomes the more significant cold-air boundary. The authors suggest a model of the principal airflows during the interaction and merging of the two cloud features and provide guidelines for the prediction of the development sequence.

Rapid cyclogenesis has been observed in some cases of interaction between comma clouds and polar-front cloud bands. Mullen (1983) documented an extremely rapid central-pressure fall (22 mb in 12 h) in a storm that occurred over the Pacific Ocean. In a paper by Businger and Walter (1988), satellite imagery revealed that four separate comma-cloud systems evolved from a region of enhanced convection associated with a cold-core 500-mb trough and a region of enhanced PVA (see Fig. 6). The development of a wave cyclone was triggered when the comma clouds and the associated upper-level short-wave trough approached a preexisting polar-front cloud band. Satellite imagery showed one of the comma clouds (labeled A in Fig. 8a) to be absorbed by the cyclone, concurrent with a cyclone central-pressure drop of more than 25 mb in 12 h. The satellite image for 0200 UTC on 14 March showing the interaction of the mature wave cyclone and the comma cloud is given in Fig. 8a. The corresponding surface-pressure analysis is given in Fig. 8b.

#### *4. Arctic-front type*

Arctic fronts, separating modified and unmodified boundary-layer air, appear to play a significant role in the formation of some polar lows, even in the absence of significant PVA. Despite the nomenclature used in this section, it should be noted that Arctic fronts are not usually analyzed on operational weather maps. This may be due, in part, to the lack of observational data in their vicinity, and, in part, to varying degrees of sharpness of the associated baroclinicity. Favored regions of formation of Arctic fronts are the Greenland, Norwegian and Barents seas, and the area south and east of Iceland. Arctic fronts also commonly occur over the Bering Sea and the northern Gulf of Alaska (e.g., Businger 1987). The regions referred to above are all located along the ice margin, where relatively warm, open water lies adjacent to ice fields or cold continents. In these regions, strong low-level baroclinicity exists

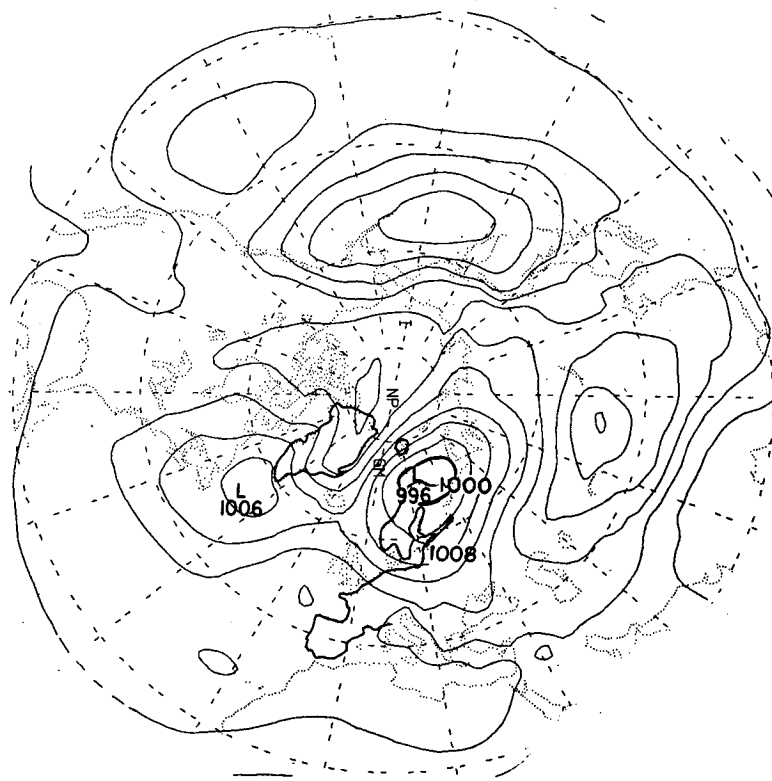


FIG. 3. Composite charts of (a) surface pressure and (b) 1000–500 mb thickness for 52 cases (1971–1982) of polar lows in the Norwegian Sea (from Businger 1985).

due to differential heating of the boundary layer over open water and over ice covered surfaces. This low-level baroclinicity appears to play an important role in the formation of polar lows that occur in conjunction with outflows of surface air from ice and snow covered regions over open water. These outflows are characterized by the presence of cloud streets in the boundary layer (Anderson et al. 1969; Brown 1980; Businger 1985 and 1987).

Figure 9 shows a cross section prepared from drop-windsonde and aircraft traverses along a line perpendicular to an Arctic front just west of Spitzbergen on 14 February 1984, during the Arctic Cyclone Experiment (Shapiro and Fedor 1986). This cross section shows the structure of the boundary-layer front and its associated low-level jet stream above the ice edge just west of Spitzbergen. Figure 9a shows the front sloping upward from the sea surface to 860 mb. The front contained a  $5^{\circ}\text{K}$  thermal gradient over 80 km, and a jet stream of  $\approx 30 \text{ m s}^{-1}$  from the northwest above the baroclinicity of the boundary-layer front. The boundary-layer inversion between  $12^{\circ}$  and  $17^{\circ}\text{E}$  was elevated by the upward flux of sensible heat on air parcels traveling within the convectively overturning boundary layer over the open water to the west of Spitzbergen. The frontal zone also contained large relative and potential vorticity (Fig. 9b), that may have played an

important role in the evolution of two Arctic lows that formed on the southern edge of the Arctic front.

The formation of boundary-layer fronts through differential heating is not restricted to the west coast of Spitzbergen. Similar structures may form when the wind flow is approximately parallel to adjacent snow- or ice-covered and open-water surfaces. These fronts can maintain their identities when changing synoptic winds advect them out to sea, despite the modifying effect of the diabatic heating by the underlying open water. Arctic fronts can often be traced from their origin at the ice edge and propagate as far away as the coast of Norway (Shapiro and Fedor 1986).

A prominent class of polar low that can be of the Arctic-front type, is the “reversed-shear” disturbance commonly found over the seas to the west and north of Norway. Reversed-shear refers to a situation in which the storm motion (or wind at the steering level) is in the direction opposite to the thermal wind, unlike the situation that prevails with the comma cloud type which propagate in the direction of the thermal wind. Duncan (1978) was first to identify the reversed-shear case and to elucidate the structure and dynamics of these disturbances.

A particularly striking example of reversed-shear Arctic lows (Reed and Duncan 1987), involving a succession or train of four disturbances that formed



FIG. 3. (Continued)

during a 2-day period, is shown in Figs. 10–12. Figure 10 shows a NOAA-7 infrared satellite image of two of the lows (labeled 3 and 4) at 1255 UTC 31 January 1983. The disturbances are spaced about 500–600 km apart and are moving southwestward at about  $5 \text{ m s}^{-1}$ .

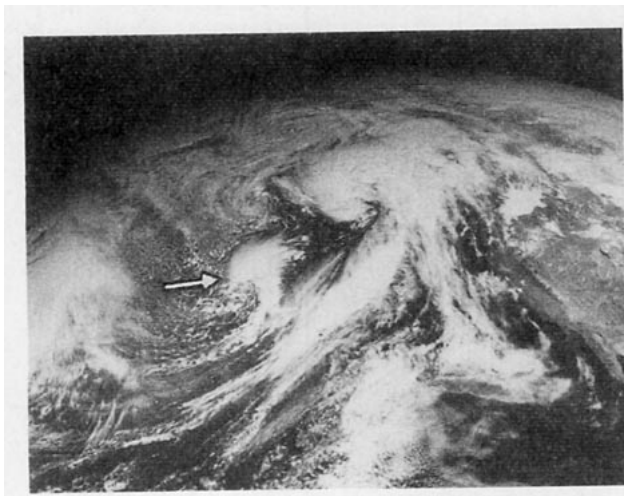


FIG. 4. The GOES visible satellite image of small comma cloud (see arrow) located to the west of a synoptic-scale frontal cyclone. The length of the arrow is  $\approx 400 \text{ km}$ . The West Coast of the United States is visible on the right-hand side of the image (from Reed 1979).

Representative constant pressure charts for the period appear in Fig. 11. It is evident that the lows are being steered southwestward in conformity with the low-level winds and that the latter are strongest near the surface where the thermal gradient is also strongest. From the orientation of the isotherms (Fig. 11a and b), it is apparent that the thermal wind is directed opposite to the low-level flow. Figure 12 depicts a cross section taken along the line AB in Fig. 11. The storm track is located near the low-level jet core. An increasingly deep layer with a near-adiabatic lapse rate extends outward from the ice edge to the vicinity of the storm track. It is clear that the Arctic lows are forming within a shallow baroclinic zone of small static stability and that the thermal contrast is produced at least in part by differential surface heating. Air to the north flows mainly over the ice and experiences little heating; air to the south flows over relatively warm water and is strongly heated and moistened from below.

The reversed-shear case is further illustrated in Fig. 13 where it is contrasted with the forward-shear type represented by the short-wave/jet streak systems. In both cases the upward motion and comma-shaped cloud pattern are located, in conformity with the Sutcliffe development principle (Sutcliffe and Forsdyke 1950), where the thermal wind advects positive vorticity, i.e., down-shear of the trough. However, because of the opposite relationships between thermal winds

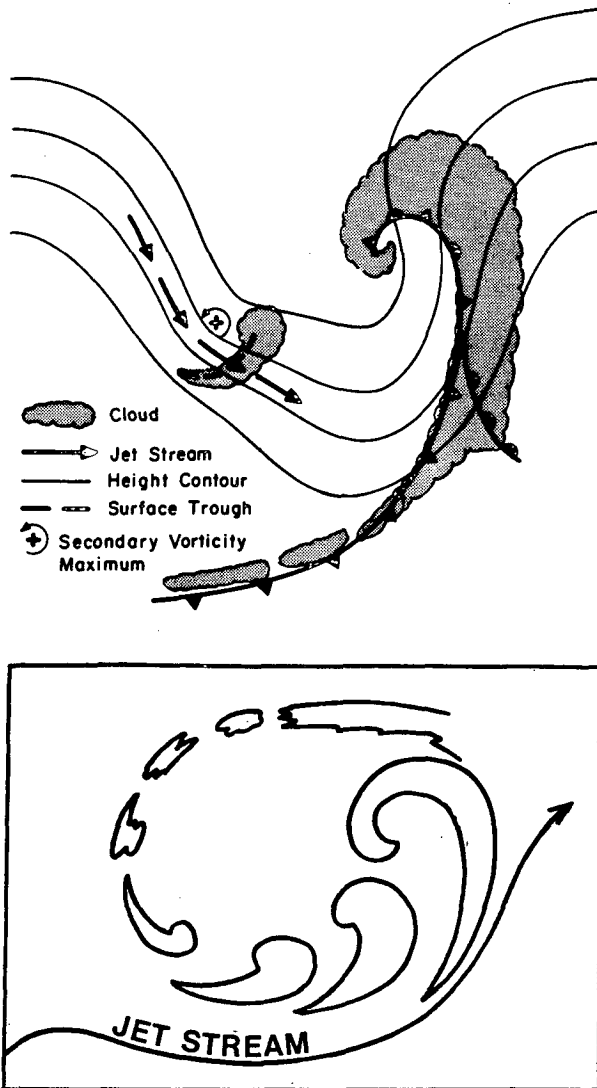


FIG. 5. (a) Schematic diagram showing typical relationship of comma cloud to major frontal cyclone and upper-level jet. (b) Schematic depiction of the principal life cycle of a comma cloud from the incipient stage to the mature vortex (from Zick 1983).

and steering level winds, the cloud system lies ahead of the trough in one case and to its rear in the other case. In some cases (Grønås, et al. 1986b) the reversed-shear disturbances appear to initiate in a tongue of warm air that protrudes northward over the open sea to the west of Spitzbergen and Bear Island.

### 5. Cold-low type

Sometimes small comma- or spiral-shaped cloud patterns of convective character are observed to flare up within the inner cores of old occlusions or cold lows, without any obvious association with upper-level short waves or low-level baroclinic features. In particular, several interesting polar lows have recently been

reported over the warm Mediterranean Sea (an otherwise unusual location for polar-low type developments), beneath cold-core upper-level lows during late fall and winter in which baroclinic instability does not appear to play a significant role (Ernst and Matson 1983; Mayengon 1984; Billing et al. 1983; and Rasmussen and Zick 1987). Although observational data in these small storms was insufficient to give detailed accounts of their structure, synoptic data, ship reports and satellite imagery suggest that they bear a resemblance to tropical cyclones. The common characteristics include very symmetric cloud signatures in satellite imagery, vigorous cumulonimbus surrounding a clear "eye", and a band of strong winds close to the eye. Evidence indicates that cyclonic circulations are most intense at sea level, gradually weakening with increasing height. Examples of two cases of this type of polar low that occurred over the Mediterranean Sea will now be discussed and illustrated.

Ernst and Matson (1983) described a case in which a hurricane-like system formed in a decaying, old occlusion beneath an upper-level cold trough. Visible and infrared satellite images (Fig. 14) show an eye-like feature and an in-spiraling convective band. The upper-level cold low is depicted in Fig. 15 and surface maps are in Fig. 16. It is evident that an intense mesoscale vortex formed within the synoptic low as the latter decayed. A ship caught in the storm recorded a sustained wind of  $25 \text{ m s}^{-1}$ , indicating that the system well exceeded tropical storm intensity.

Another example of a hurricane-like development is described by Rasmussen and Zick (1987). As in the previous case, the development occurred in the central part of a synoptic-scale cold-core low of modest intensity, and deep convection was observed prior to the formation of the mesoscale vortex. The authors used METEOSAT imagery to observe the structure of the clouds and calculate the cloud-level winds by tracking cloud elements as the disturbance evolved. They found that deep convection preceded the formation of the vortex at the surface, and attribute the surface development to a rapid spinup of surface vorticity, associated with the parent synoptic-scale low, by the intense convection. In its mature stage, the vortex was characterized by deep convection, a vertical axis and an upper-level anticyclonic divergent outflow corresponding to a warm-core structure. At this stage, the storm had a distinct similarity to its tropical counterpart (see for example Fig. 14).

### 6. Multitype developments

The foregoing examples of short-wave and Arctic-front type of polar lows highlight two quite distinct flow patterns that are associated with polar-low development, one characterized by upper-level PVA and the other by shallow baroclinity. When an upper-level short wave traverses the marginal ice zone, it is possible

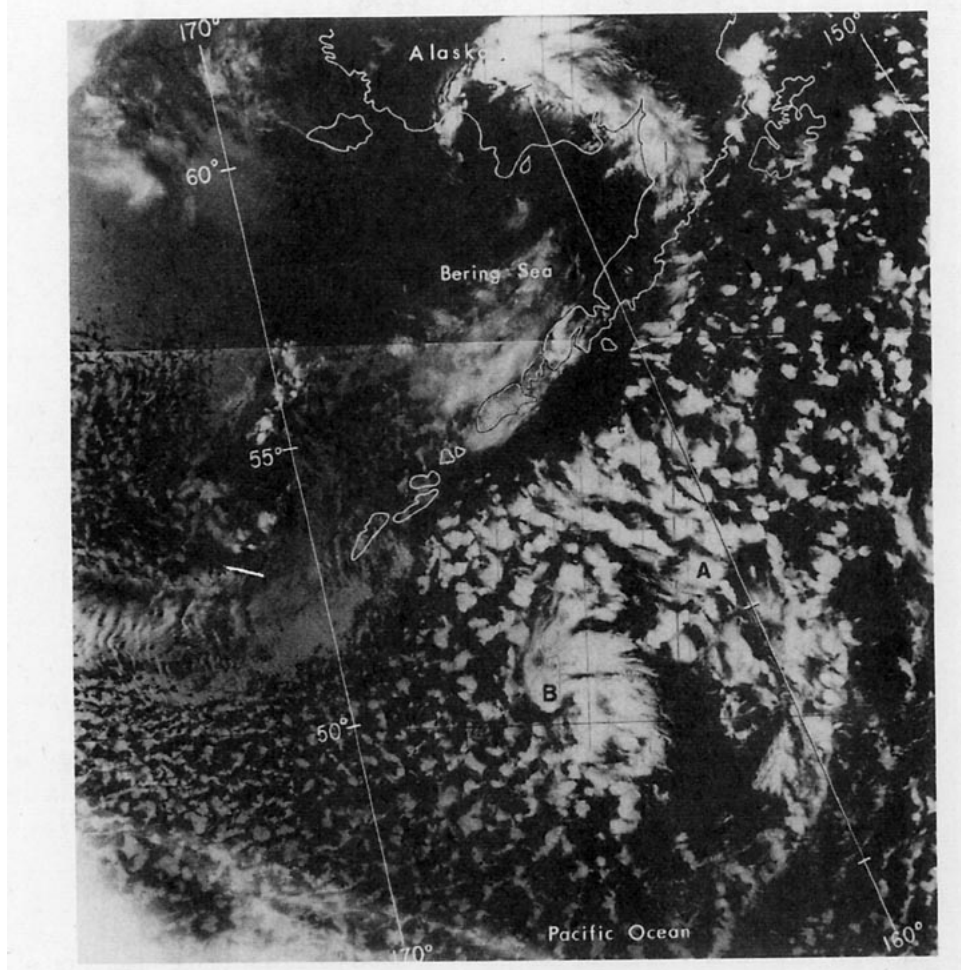


FIG. 6. The NOAA-6 infrared-satellite image of enhanced convection (A), and an incipient comma cloud (B) at 1800 UTC 12 March 1985 (from Businger and Walter 1988).

for a system to develop that combines both features. Two fascinating examples of multitype developments will now be described.

#### a. *The Bear Island case*

The first case to be illustrated developed over the Barents Sea and has been documented by Rasmussen (1985a,b). As pointed out by Rasmussen, there were two distinct stages in the development of this polar low. A satellite infrared image of the system taken at 0250 UTC 13 December 1982 is shown in Fig. 17 during the initial stage of development. At this time, a spiral-shaped cloud pattern was present. Antecedent conditions at 500 mb are displayed in Fig. 18, and a sequence of surface maps commencing at about the time of the satellite picture appear in Fig. 19.

The upper-level chart for 1200 UTC 12 December (Fig. 18b) shows a sharp trough and closed low west of Bear Island. The path of this short wave system is indicated by the broken line. It appears from the evo-

lution at 500 mb that upper-level vorticity advection played a role in the initial development. The surface chart for 0000 UTC 13 December (Fig. 19a) shows only a trough in the vicinity of the incipient low. This trough, located within the region of strong low-level thermal contrast, strengthens during the ensuing 12 h, while a well-formed comma- or spiral-shaped cloud remains on the satellite picture (not shown). The later surface charts reveal that a dramatic second stage of development took place between 1200 UTC on the thirteenth (Fig. 19b) and 0000 UTC on the fourteenth (Fig. 19c). A small, tight, surface low is seen to cross weather ship AMI located just off of the Norwegian Coast, bringing a pressure fall of 5.9 mb during a 3-h period and winds of  $20 \text{ m s}^{-1}$  within a distance of 50–100 km of the low center. The surface pressure trace for weather ship AMI during the low's passage (Fig. 20) shows a rapid pressure fall between points A and B, followed by a more gradual rise between points B and C as the low moves away from AMI. It is perhaps significant that the hurricane-like core formed as the

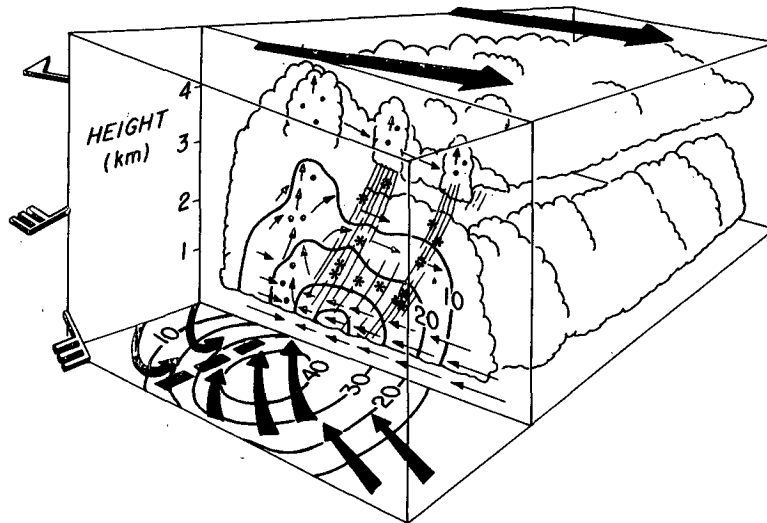


FIG. 7. Schematic depiction of a rainband in a comma cloud. The scalloped lines show the edge of the cloud. The front portion of the rainband has been omitted in order to show its microphysical structure in the vertical, the airflow relative to the band (heavy arrows), the convergence line (heavy dashed line) and radar reflectivity [solid contours marked in  $\text{dB}(Z)$ ] just above the surface. The vertical cross section also shows the airflow relative to the band (small arrows) and radar reflectivity [solid contours marked in  $\text{dB}(Z)$ ]. Also depicted are small convective cells near the top of the rainband, from which fallstreaks emanate. The microphysical structure of the rainband is indicated by the solid dots (regions of relatively high liquid water content), and hexagons (regions of relatively high ice particle concentrations). Aggregates of ice particles are depicted by overlapping hexagons. On the left side of the figure, the wind at various heights is shown (1 barb =  $5 \text{ m s}^{-1}$ , 1 triangle =  $25 \text{ m s}^{-1}$ ). The wind direction just above the top of the rainband is shown by the large heavy arrows at the top of the figure (from Businger and Hobbs 1987).

low passed over the warmest waters. Because of the upper-level vorticity advection and enhanced low-level baroclinity, this system can be classified as a combined type, but it had the added ingredient of a hurricane-like core.

#### b. The ACE case

The second example of a multitype polar low occurred during the Arctic Cyclone Expedition (ACE) of 1984 when a research aircraft successfully penetrated a mature mesoscale vortex (Shapiro et al. 1987). This resulted in the best available documentation of the structure of a small, intense polar low to date. The 1000-mb and 700-mb operational analyses from the European Centre for Medium-range Weather Forecasts for this case are shown in Fig. 21. The circled cross marks the position of the polar low. Lacking the flight data, the 1000-mb analysis gives no hint of the low. The surface pressure and 300-m winds determined from the aircraft observations appear in Fig. 22. It is seen that a small cyclone with central pressure of about 980 mb and winds near the surface in the  $25\text{--}35 \text{ m s}^{-1}$  range at radial distances of 50–100 km was present in the rear part of the synoptic-scale low. Aircraft soundings revealed that the low possessed a warm core. The satellite picture for this time (Fig. 23) shows a comma-

shaped cloud pattern with the suggestion of an eye-like feature in the head. The Arctic low was the most intense of five mesoscale vortical circulations that were observed within the general cloud shield during a period of about 12 h. Scales ranging from synoptic down to the small mesoscale appear to be involved in this notable case. Synoptic-scale lapse rates based on ECMWF analyses (Fig. 24) reveal the destabilization that occurred at the 1200 UTC 27 February position of the polar low (marked by the cross in Fig. 21b) as the upper-level trough associated with the parent low approached and passed the point.

### 7. Theoretical studies and numerical prediction experiments

In this section we will give a brief summary of some theoretical ideas and studies<sup>1</sup> and numerical modeling experiments relevant to the polar low problem that have been presented in the recent literature.

#### a. Theoretical ideas and studies

Several mechanisms exist in current instability theory that in combination or alone might explain the

<sup>1</sup> For a more complete discussion of this subject, the reader is referred to a companion article by the authors in *Polar Lows* (1989).

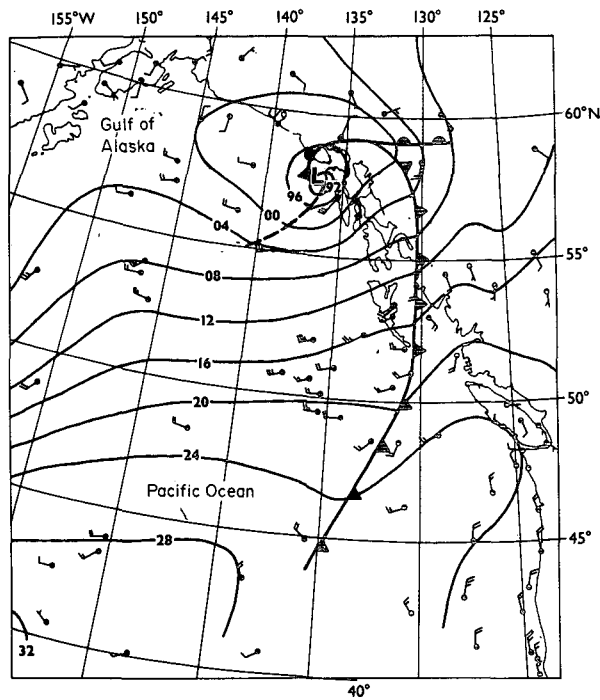
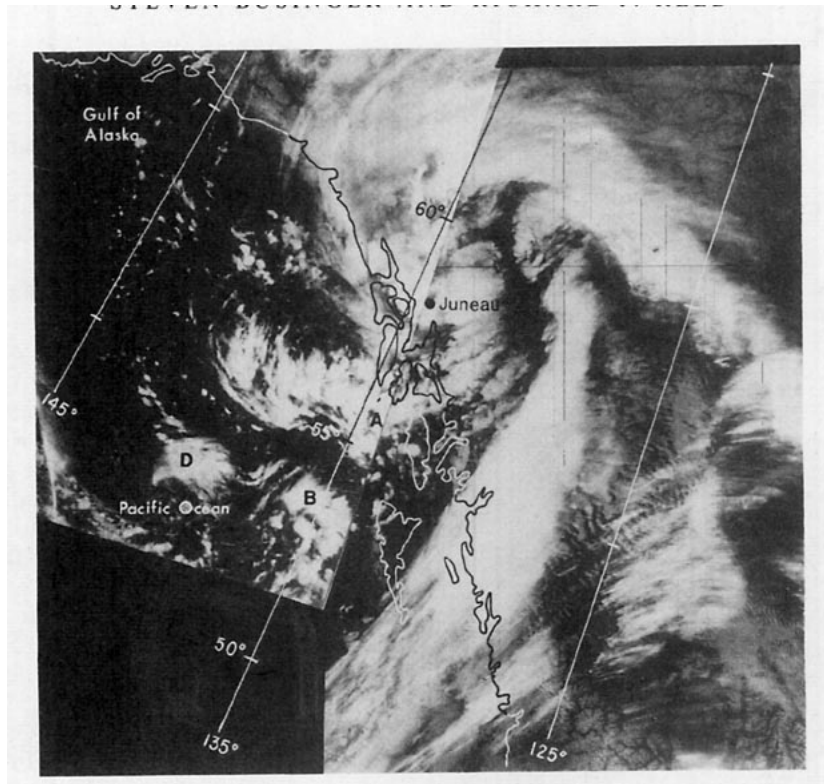


FIG. 8. (a) The NOAA-6 infrared-satellite image showing the interaction of developing comma cloud (A) and wave cyclone at 0200 UTC 14 March 1985. Lower case "c" indicates locations of enhanced convection along the occlusion cloud band (W). (B) and (D) indicate localized enhanced convection associated with mesoscale vortices in the cold air. (b) Surface-pressure analysis for 0000 UTC 14 March 1985 (solid contours are isobars every 4 mb). The heavy dashed line indicates the position of the surface through axis located to the rear of the comma cloud (from Businger and Walter 1988).

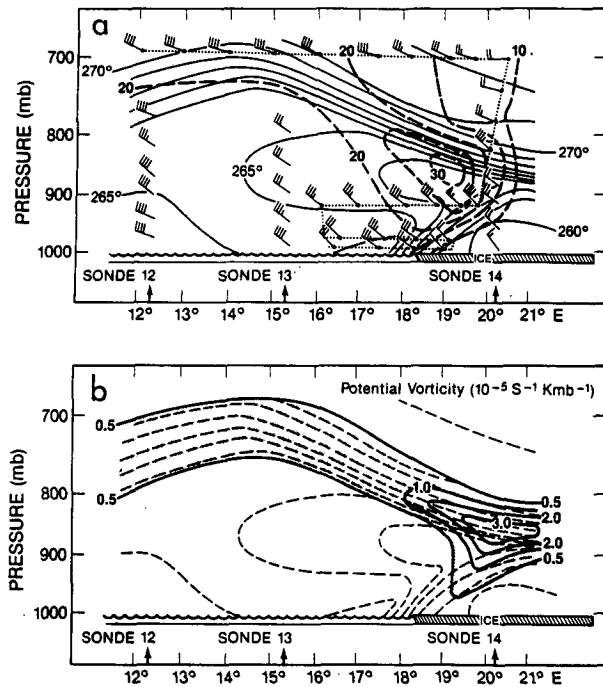


FIG. 9. Cross-sectional analyses along a line perpendicular to the ice edge west of Spitzbergen through the Arctic front on 14 February 1984: (a) Potential temperature (K, solid lines). Dropwindsonde locations indicated by heavy arrows plotted below. The dashed line indicates the aircraft flight track. Wind vectors without dotted heads show the dropwindsonde wind profiles; wind vectors with flag,  $25 \text{ m s}^{-1}$ ; full barb,  $5 \text{ m s}^{-1}$ ; and half barb,  $2.5 \text{ m s}^{-1}$ . (b) Solid lines indicate potential vorticity (in units of  $10^{-5} \text{ s}^{-1} \text{ mb}^{-1}$ ) and dashed lines indicate potential temperature. Stippled areas show potential vorticities in the range  $(0.5-2.0) \times 10^{-5} \text{ s}^{-1} \text{ mb}^{-1}$  (from Shapiro and Fedor 1986).

formation and/or intensification of polar lows. They include: (i) baroclinic instability, (ii) conditional instability of the second kind (CISK), (iii) air-sea interaction instability, and (iv) barotropic instability.

### 1) BAROCLINIC INSTABILITY

The presence of significant baroclinicity through a considerable depth of the troposphere in the vicinity of polar lows, as revealed by a number of studies (Harley 1960; Harrold and Browning 1969; Mullen 1979; Reed 1979; Locatelli et al. 1982), supports the view that baroclinic instability can play a primary role in the formation and intensification of polar lows.

Interest in baroclinic instability as a factor in polar-low formation was much stimulated by Harrold and Browning's well-known paper (1969). Using radar, these authors showed that in the case of a polar low passing over England the precipitation occurred mainly in slantwise ascent as in a typical baroclinic disturbance. On the basis of a cursory inspection of several small comma cloud developments over the Pacific Ocean, Reed (1979) stated that these systems invariably

form in the cyclonic-shear zone poleward of the jet stream and that this zone is marked by conditional instability and weak to moderate baroclinity. Mullen (1979) obtained a composite picture of the large-scale environment of 22 small comma clouds that formed over the Pacific Ocean that reinforced the foregoing description and interpretation. Locatelli et al. (1982) showed that the mesoscale structures of several larger comma clouds exhibited wind, temperature, and precipitation patterns similar to those observed in larger extratropical cyclones that form on the polar front. Reed (1979) pointed out that relatively intense comma clouds can develop in polar air masses over land (e.g., see Wallace and Hobbs 1977, p 110; Mullen 1982) in the absence of significant sensible-heat and moisture fluxes from the surface, which indicates that the potential energy released by baroclinic instability alone might be sufficient to account for the development of some polar lows.

A succession of theoretical papers dealing with baroclinic instability as a mechanism of polar low formation using numerical models have followed Harrold and Browning's work. These include: Mansfield (1974); Duncan (1977, 1978); Staley and Gall (1977); Blumen (1980); and Orlanski (1986). In brief, the model results highlight the importance of small static stability at low levels and moist processes in promoting vigorous development in a baroclinic environment.

Reed and Duncan (1987) have recently applied the dry baroclinic model of Duncan (1977) to the observed background state in the case of the train of four, more or less evenly spaced polar lows described in section 4. Their computations yielded a wavelength of maximum instability that was consistent with the observed wavelength of 500–600 km, suggesting a possible baroclinic origin for the wave train. These authors pointed out, however, that some factor other than baroclinity—presumably latent-heat release in deep convection—must have been an important factor in the development, since the observed lows moved at significantly slower speeds than predicted by the dry-baroclinic model and the growth rates given by the model, though substantial, were not sufficiently large, especially in view of the neglect of friction.

The above cited baroclinic studies using dry models all yield unrealistically shallow structures. That latent heat release can have a profound effect on the structure and growth of polar lows is evident from the work of Gall (1976). In studying baroclinic wave growth, he found that the effects of condensational heating are to increase amplitudes near 500 mb, where cloud signatures suggest that considerable rotation exists, and to increase the growth rate of short waves.

### 2) CONDITIONAL INSTABILITY OF THE SECOND KIND (CISK)

Paralleling the studies of the role of baroclinic instability in polar low development have been a number



FIG. 10. The NOAA-7 infrared satellite image of two polar lows (Nos. 3 and 4) at 1255 UTC 31 January 1983 (adapted from Rasmussen and Lustadt 1987).

of studies that have examined quantitatively the role of diabatic processes. The underlying concept in most of these studies has been that of conditional instability of the second kind (CISK) introduced by Charney and Eliassen (1964) to explain the growth of the hurricane depression. The CISK theory explains their growth as the result of a cooperative interaction between cumulus convection and large-scale circulation. The CISK process occurs if the convection becomes sufficiently organized, so that a positive feedback develops between the cloud scale and the developing vortex scale, in which the vortex-scale motion provides moisture convergence for the convective process and the cumulus-scale provides latent heating that intensifies the large-scale disturbance. Results from analytical numerical models (Økland 1977, 1987; Rasmussen 1977, 1979; Bratseth 1985) make it apparent that the CISK mechanism can be a vital factor in polar low development.

The combined effects of baroclinicity and CISK have been studied by Sardie and Warner (1983) with the use of a three-layer, two-dimensional, quasi-geostrophic model, which included both the effects of latent heating and baroclinity. They found that, in general, both moist baroclinity and CISK were of importance in polar low formation, though moist baroclinic processes alone were sufficient to account for the comma cloud type of development. Prior to Sardie and Warner's work, most investigators emphasized either baroclinic insta-

bility or diabatic heating as the primary cause of polar low development. Lately there seems to be greater recognition that the interaction of both mechanisms needs to be taken into account.

### 3) AIR-SEA INTERACTION INSTABILITY

Although widely cited as an explanation for the development of hurricanes, CISK is a conceptual model that does not directly address the storm dynamics. Objections to the CISK model have recently been voiced by Emanuel (1986), who states: "the average generation of convective available potential energy (CAPE) in the tropical atmosphere by radiation and sea-surface fluxes is apparently just enough to balance the dissipation of kinetic energy within cumulus clouds, and without augmentation could not account for the greatly increased dissipation of kinetic energy in the hurricane boundary layer." Furthermore, numerical experiments (Ooyama 1969; Rosenthal 1971) clearly show the crucial importance of heat fluxes through the sea surface. As an alternative to CISK, Emanuel (1986) has proposed that tropical cyclones result from an air-sea interaction instability in which anomalous sea-surface fluxes of sensible and latent heat induced by strong surface winds and falling pressure, lead to increased temperature anomalies, and thereby to further increases in surface winds and pressure deficit. He shows, using

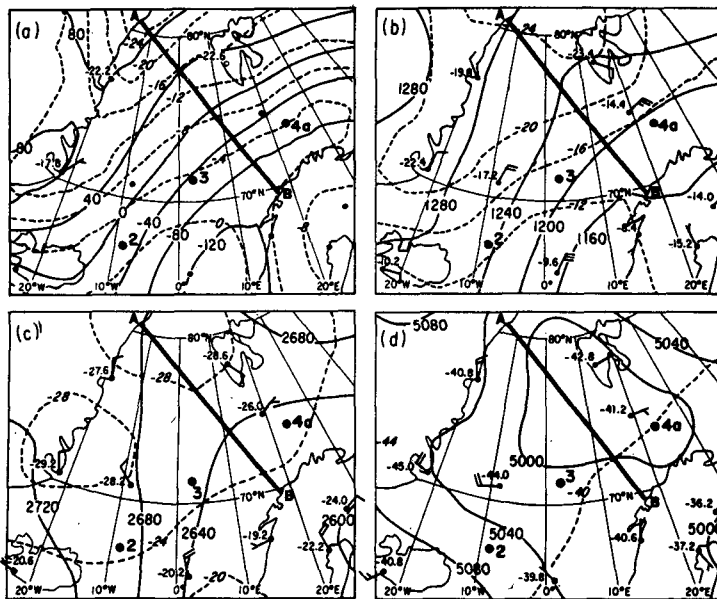


FIG. 11. The (a) 1000-mb, (b) 850-mb, (c) 700-mb, and (d) 500-mb charts for 1200 UTC, 30 January 1983. Solid lines contour at 40-m intervals; dashed lines isotherms at 4°C intervals. Numbered dots indicate positions of polar lows (from Reed and Duncan 1987).

a simple nonlinear analytical model, and an axi-symmetric numerical model, that this hypothesis is consistent with observations of tropical cyclones.

The possible significance of an air-sea interaction mechanism for cyclogenesis in polar air masses be-

comes apparent in light of the large fluxes of sensible and latent heat into the boundary layer of incipient polar lows measured during the Arctic Cyclone Experiment (ACE). Data indicate that combined fluxes of sensible and latent heat may have been as high as

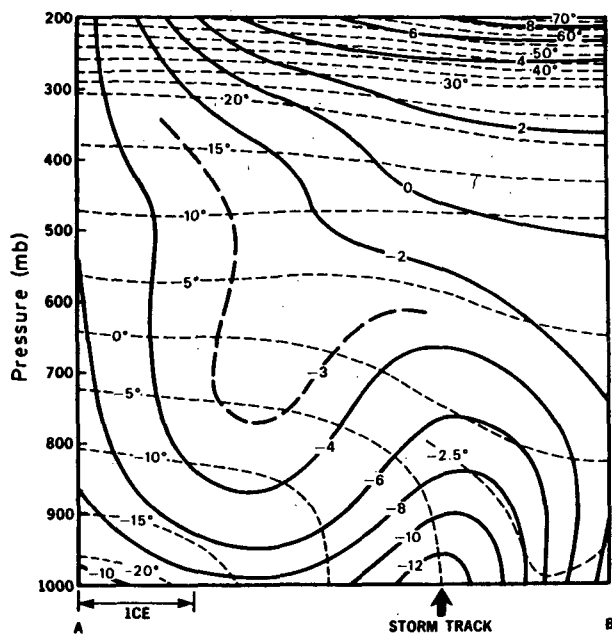


FIG. 12. Cross section along line AB in Fig. 11. Solid lines are isochets ( $m s^{-1}$ ). Dashed lines are potential isotherms ( $^{\circ}C$ ) (from Reed and Duncan 1987).

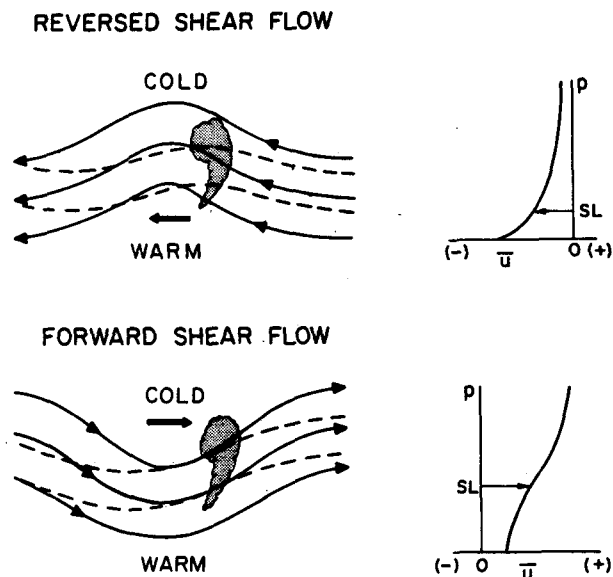


FIG. 13. Comparison of structures of disturbances in reversed-shear flow (top) and forward-shear flow (bottom). Solid lines, streamlines; dashed lines, isotherms at the steering level. Heavy arrows, phase propagation vector and steering level (SL) wind. Stippling, comma cloud.



FIG. 14. (a) The NOAA-7 visible image 1236 UTC 26 January 1982; numbered arrows indicate location of 1) Yugoslavia, 2) Albania, 3) Hungary, 4) Romania, 5) Italy, and 6) polar low; (b) NOAA-7 enhanced infrared image for same time (from Ernst and Matson 1983).

1000 W m<sup>-2</sup> over the Norwegian Sea during the development of a particularly intense Arctic low (Shapiro et al. 1987) (see section 6.2). This value is comparable to the heat fluxes observed in hurricanes. As Rasmussen and Lystad (1987) have pointed out, however, CAPE is large in the cold air outbreaks within which polar lows develop, and therefore, the arguments applied to the tropical hurricane may not apply to the Arctic systems.

Emanuel and Rotunno (1988) tested Emanuel's air-sea interaction mechanism for polar lows by using

conditions observed in the atmosphere over the Norwegian Sea prior to a complex polar-low development documented by Rasmussen (1985a,b) (see section 6.1). This case was chosen in part because of the nonadvective warming seen at the core of the polar low. Results from Emanuel's calculations using a simple nonlinear analytical model, and an axisymmetric numerical model, show that the air-sea interaction hypothesis is consistent with observed Arctic low development, but requires a preexisting disturbance to act as a triggering mechanism before the air-sea interaction instability can operate. This two-stage development is consistent with evidence for two stages in the deepening of this disturbance. However, the rate of deepening calculated numerically is less than that observed; this is a discrepancy that requires further study.

#### 4) BAROTROPIC INSTABILITY

Mullen (1979) showed that the necessary condition for barotropic instability generally is met in areas conducive to the development of comma clouds. As first discussed by Reed (1979), however, it appears very unlikely that a jet stream could be narrow enough to account for the mesoscale and small-synoptic scale wavelengths observed in polar lows, if barotropic processes alone are responsible. Reed's observation is consistent with Sardie and Warner (1985), who show that a jet maximum of 80 m s<sup>-1</sup> with a half-width of 5° latitude would result in a growth rate of  $\approx 1.6 \times 10^{-6}$  s<sup>-1</sup>. This very small rate implies that, although the necessary condition for barotropic instability is met, it cannot be an important contribution to disturbance

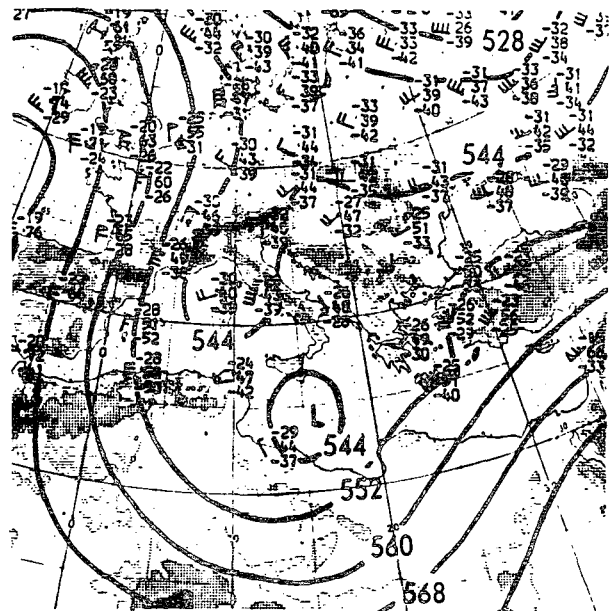


FIG. 15. The 500-mb chart, 0000 UTC 25 January 1982 (from European Meteorological Bulletin).

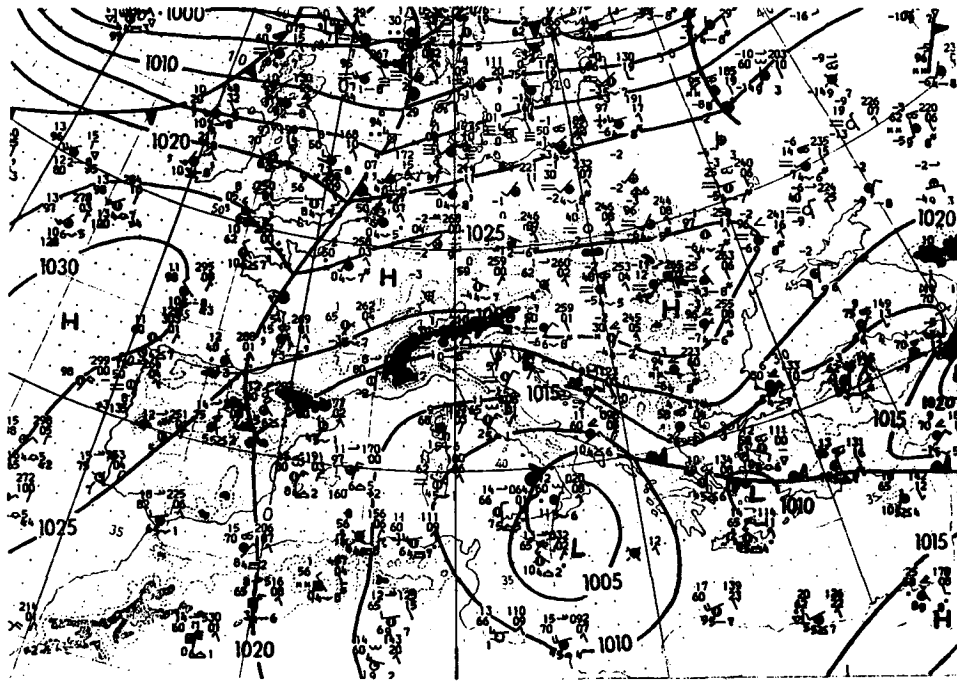


FIG. 16. Surface maps: (a) 1200 UTC 25 January 1982, and (b) 1200 UTC 26 January 1982 (from European Meteorological Bulletin).

growth. It is interesting to note, however, that disturbances developing in a flow that is both baroclinically and barotropically unstable, tend to have maximum geopotential perturbation at the jet-stream level, while those that are barotropically damped tend to have a maximum near the surface (Mudrick 1974).

In conclusion, although barotropic instability is present in many polar low developments, calculations indicate that it represents only a minor contribution to the rapid development observed in polar lows.

#### *b. Numerical prediction experiments*

We review here briefly the few prediction experiments that have been carried out using observed initial data and mesoscale models of sufficiently fine resolution to at least roughly represent systems of the dimensions of polar lows. Comments concerning the operational application of numerical prediction models to the problem of forecasting polar lows will be deferred to section 8. Information concerning the models, the cases investigated and the data sources is given in Table 1 for simulations conducted by Seaman (1983), Sardie and Warner (1985), Grønås, Foss and Lystad (1986a,b, 1987), and Nordeng (1987). The two models utilized thus far, the Pennsylvania State University/National Center for Atmospheric Research (PSU/NCAR) and the Norwegian Meteorological Institute (NMI) mesoscale models, are advanced models that represent the basic physical processes believed to be of importance in polar-low development. The processes include sur-

face and boundary layer fluxes and release of latent heat by resolvable motions (explicit convection) and by parameterized, subgrid-scale convection.

Short-range (12-h) forecasts obtained by Seaman were moderately successful, though they underestimated the intensity of the disturbance. Surface fluxes, convection and forcing by an upper-level short-wave all proved necessary for the maintenance of the storm. The Atlantic low investigated by Sardie and Warner developed baroclinically at first, but latent heat release and surface fluxes were required for its subsequent maintenance. The Pacific low was well predicted in the control experiment that employed parameterized convection. Baroclinicity was identified as the major factor in the deepening, however, since latent heat release accounted for only 5 mb of a total of 14 mb deepening. An experiment using explicit convection produced a significant overintensification, a common feature of the explicit scheme, at least in earlier studies.

In all cases studied by Grønås et al., disturbances were predicted that could be associated with the observed polar lows. A failure of the forecasts was their inability to predict the strength of the disturbances when the scale was small. The low investigated by Shapiro et al. (1987) was a case in point. The failure may arise from a lack of sufficient resolution in the model to capture essential features of the initial state or to represent essential physical processes.

Nordeng (1987) has developed a parameterization method for slantwise convection in the Norwegian

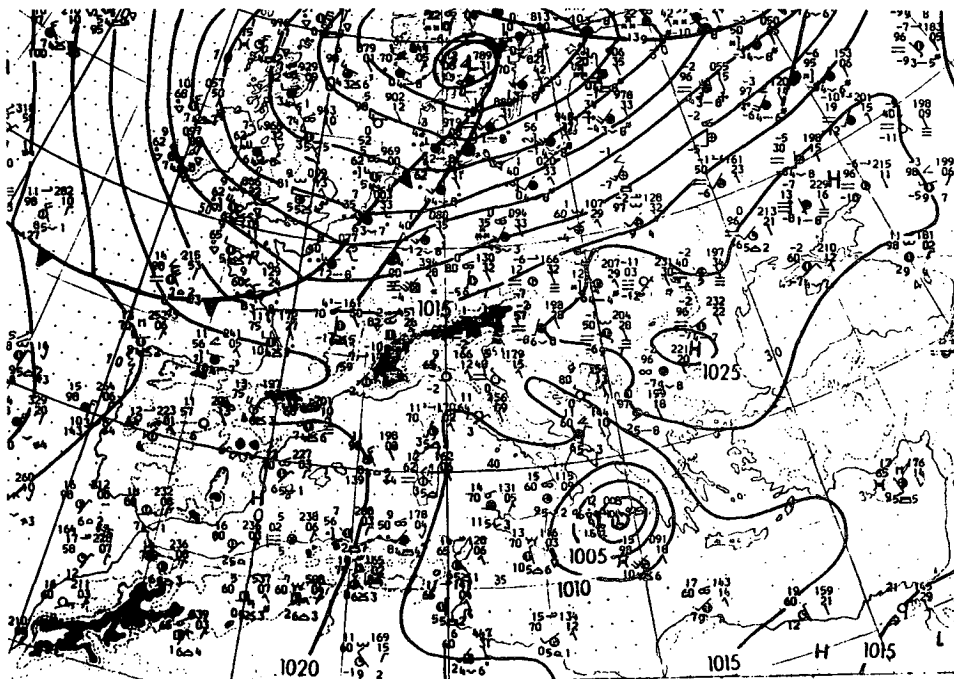


FIG. 16. (Continued)

Meteorological Institute (NMI) mesoscale model. Although the potential of his parameterization scheme is clear, the forecasts made with the revised model were still unable to reproduce the magnitude of the surface deepening observed in the polar-low cases simulated, a shortcoming he attributes to the small scale of polar-low developments and the modest 50-km grid-point resolution of the model.

**8. Forecasting polar lows**

The numerical simulations described in section 7, carried out with real data but in the research mode, demonstrate the ability of advanced mesoscale models to forecast polar lows with at least some degree of success in a variety of situations and locations. In this section we address the more relevant question of the performance of operational forecast models in predicting polar lows. After noting the capabilities and limitations of the operational models, we describe some forecast methods developed by Norwegian meteorologists that use model output in conjunction with other sources of information, particularly satellite data, as a means of dealing with the practical problem of forecasting polar lows. Because of the previously emphasized range of sizes and structures that characterizes these systems, the success of operational models depends greatly upon the type of low being considered. Accordingly, it is convenient to discuss model performance in terms of the types identified in sections 3-6.

Considering first the short-wave, jet-streak type, we can assert on the basis of everyday experience that these systems at the larger end of the size spectrum are usually handled with some measure of success by current operational models (e.g., the NMC spectral and NGM models). We are unaware of any verification studies that have been carried out to test this assertion, but we can point to specific examples, for instance, the two cases examined by Reed and Blier (1986a,b) in which the systems can be identified in both the initial and the prognostic fields. These cases also furnish examples of the tendency of the models to underpredict this type of development (but not as badly as for some of the other types).

The comparative success of the operational models in predicting the upper-level, short wave type stems from the ability of the analysis systems to capture the upper-level vorticity maxima and jet streaks that are crucial to their development. Some of the vorticity maxima have long histories, being remnants of earlier synoptic-scale disturbances. Others seem to form when a lobe of high vorticity protrudes outward from a pool of cyclonic relative vorticity contained within a large upper-level cold low. In either case, the characteristic field of enhanced convection, which later becomes organized in a comma-shaped pattern, appears in the PVA region ahead of the upper-level vorticity maximum.

The Arctic-front type of polar low presents a much more difficult forecast problem. Because of its small



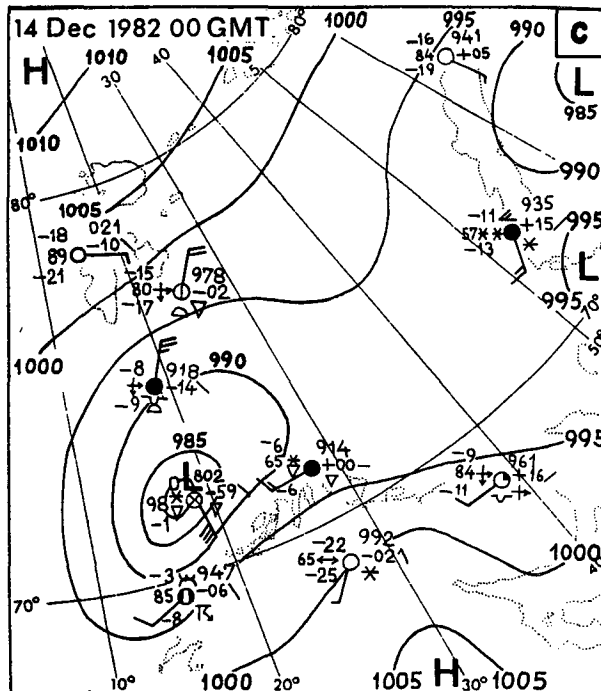
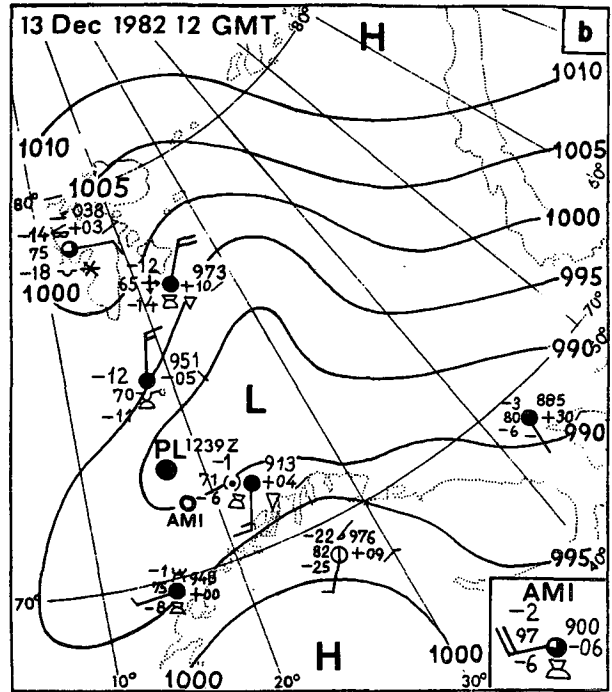
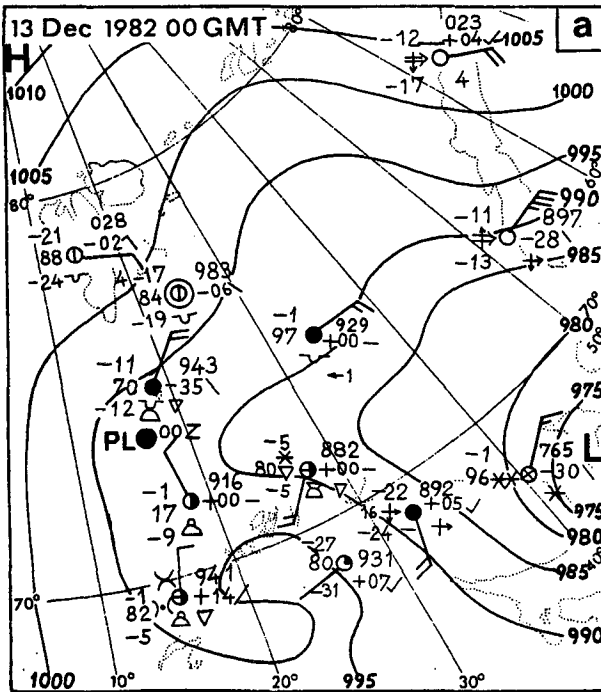


FIG. 19. Surface maps for (a) 0000 UTC, and (b) 1200 UTC 13 December 1982, and (c) 0000 UTC 14 December 1982 (contours every 5 mb). Here "PL" indicates position of the polar low (from Rasmussen 1985a).

In the case of the multitype developments described in section 6, some predictive skill is possible, since they involve identifiable migratory upper-level vorticity maxima as well as a favorable lower-level environment that is at least partly resolvable by the model. The larger-scale features of the Bear Island and the ACE

cases discussed in section 6 (Figs. 19a, b and Fig. 21, respectively) that could be associated with upper-level PVA were predicted by the numerical forecasts. However, the second stage of development in these cases, featured by the appearance of small, intense vortices (Figs. 19c and 22), was essentially unpredictable be-

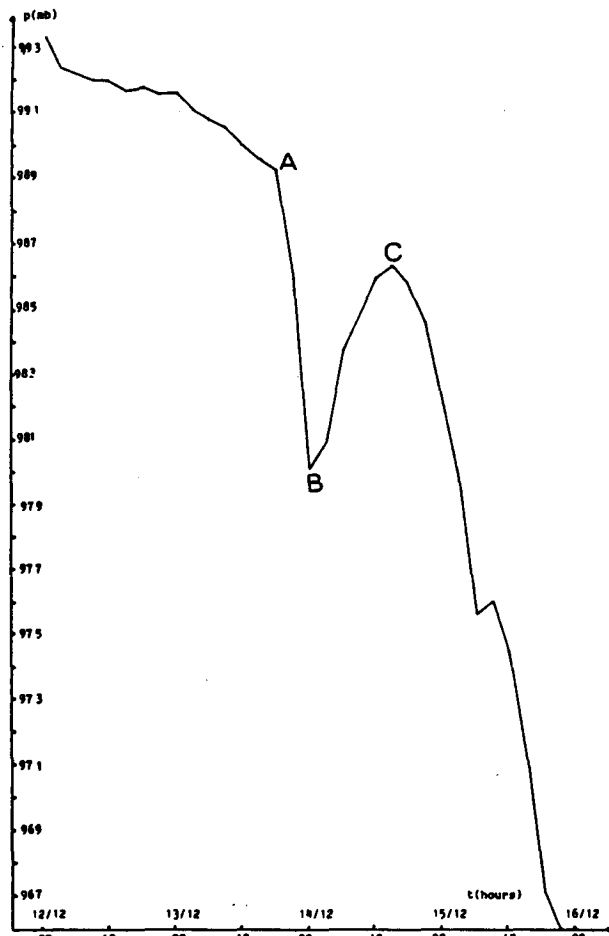


FIG. 20. The surface pressure at AMI as function of time from 12-16 December 1982 (from Rasmussen 1985b).

cause the initial part of the rapid-intensification phase could not be uniquely associated with the upper-level forcing (each of the vortices was only one among a number of small vortices) and because at later stages the vortices could not be adequately resolved by the observing network and forecast system.

Given the limited usefulness of the operational models in the prognosis of polar lows, How should the forecaster deal with the prediction problem? This question was addressed by Norwegian meteorologists in connection with the Polar Lows Project that was conducted in the Norwegian and Barents seas between January 1983 and December 1985 (Lystad 1986). On the basis of their experience, the investigators divided the problem into two parts: the problem of monitoring, which involves the synthesis of all available data into the most probable representation of the atmospheric state, and the problem of making the actual forecast. There were three elements in the monitoring: the first was the use of analyses based on model assimilated data; (A fine-mesh, 50-km grid model was employed

in the assimilation;) the second was attention to individual reports from land, ship, and drifting buoy locations and radiosonde stations; and the third, and most important, was interpretation of infrared images from polar orbiting satellites. Because of the characteristic under prediction of the intensity of the lows by the model, subjective corrections were made to the numerical analyses when the other sources of information suggested the presence of a polar low.

Forecasting methods were developed and tested during the Polar Lows Project (Lystad 1986) that treated both the problem of identifying areas of likely polar-low development, without attempting to pinpoint

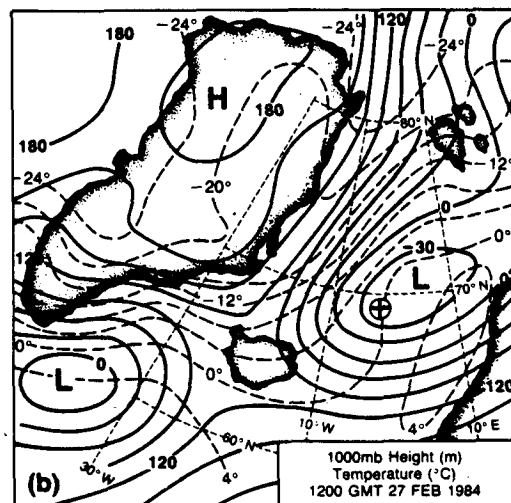
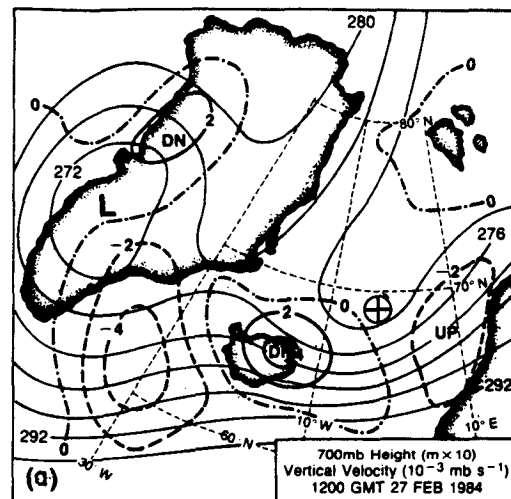


FIG. 21. The ECMWF analyses for 1200 UTC 27 February 1984: (a) 700-mb heights (thin solid lines in dm); and vertical velocity ( $10^{-3} \text{ mb s}^{-1}$ , heavy dashed lines are positive, heavy dot-dash lines are negative). (b) 1000-mb heights (solid lines in m) and isotherms (dashed lines in  $^{\circ}\text{C}$ ). Circled cross marks position of the polar low (from Shapiro et al. 1987).

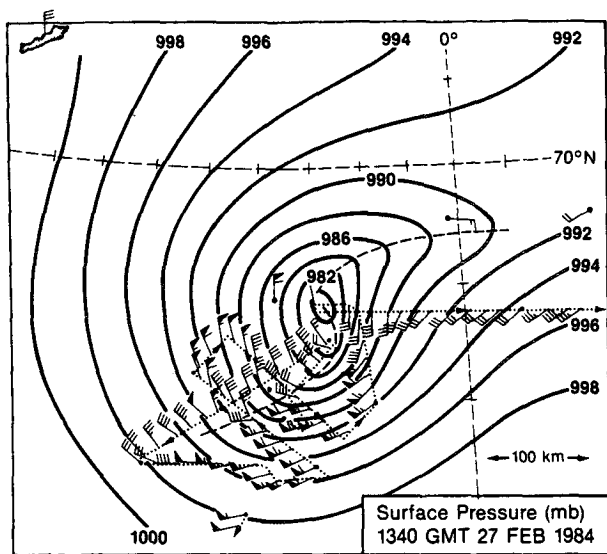


FIG. 22. Surface pressure (mb) and 300-m winds at 1340 UTC 27 February 1984. Full barb,  $5 \text{ m s}^{-1}$ ; and pennant,  $25 \text{ m s}^{-1}$  (from Shapiro et al. 1987).

the actual locations of the storms, and the problem of predicting the track of a low in cases where one was detected. The method for selecting areas with significant probability of polar-low occurrence made use of three simple criteria: 1) cold air advection at the sea surface, 2) 850–500 mb thickness of less than 3960 m (adjusted according to the sea surface temperature), and 3) cyclonic or zero curvature of contours at 500- and 700-mb levels. In 2.5 months of operational testing this method was successful in identifying all cases of polar-low occurrence. The method, however, also forecast about the same number of cases in which polar

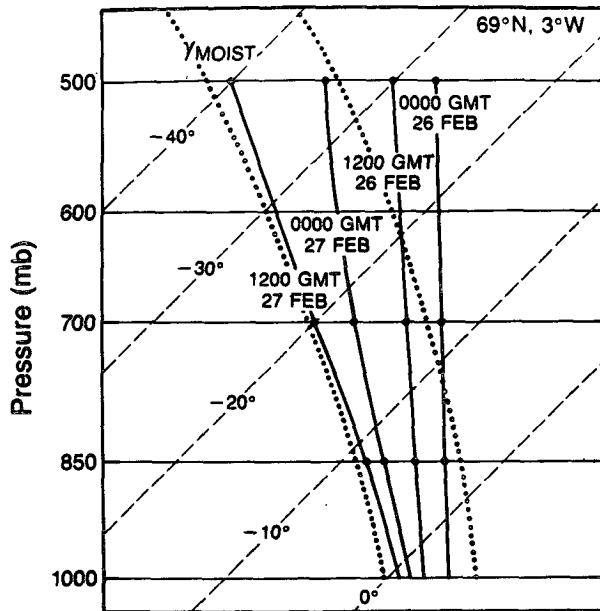


FIG. 24. Temperature profiles (heavy solid lines) over the region of polar-low development ( $69^\circ\text{N}$ ,  $3^\circ\text{W}$ ) for the period 0000 UTC 26 February–1200 UTC 27 February 1984 (from Shapiro et al. 1987).

lows failed to appear. Clearly, fine-tuning of the method is required before it can be regarded as fully useful.

The best method for predicting the tracks of already identified lows proved to be construction of storm paths from model-predicted 850- and 700-mb winds under the assumption that the systems are steered by the winds at these levels. Testing of the method using 850 winds revealed an average position error for 18-h forecasts of 200 km compared with a mean path length of 800 km (Midtbø 1986). Though developed for the Norwegian and Barents sea areas, the foregoing forecast methods could with modification be applied to other regions.

What does the future hold for polar low prediction? Opportunities exist for better monitoring of the lows that could lead to a significant enhancement of predictive skill. In the case of satellite observations, scanning passive microwave radiometers that measure total water vapor content and, more importantly, precipitation rate in an atmospheric column (McMurdie and Katsaros 1985), provide a new tool for better detection of polar lows. In addition, microwave scatterometers give promise of yielding high-resolution surface wind fields. The high temporal frequency needed to observe rapidly developing storms, which cannot be obtained from polar orbiting satellites, may, at least in some areas, be achievable for geostationary orbit with use of an image processing technique developed by Zick (1986) that stretches the high latitude portions of the satellite picture. Obviously, deployment of an increased number of drifting buoys and of coastal radars are steps

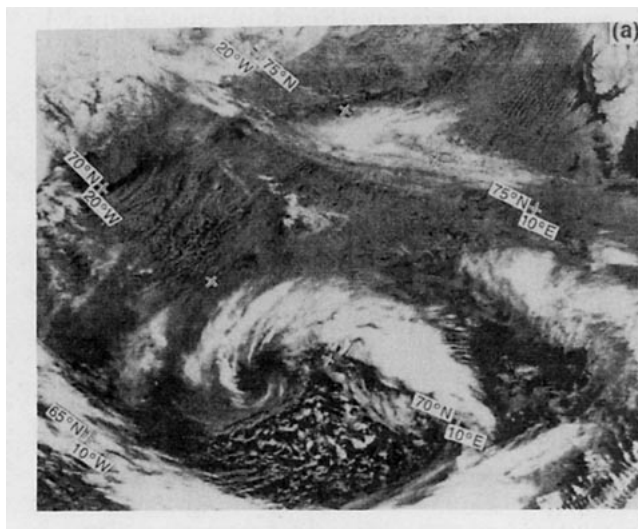


FIG. 23. The NOAA-7 satellite infrared image for 1340 UTC 27 February 1987 (from Shapiro et al. 1987).

TABLE 1. Polar-low simulations using full physics mesoscale models and observational data.

Investigators	Model	Resolution (km)	Layers	Cases	Area	Sources
Seaman (1983)	PSU/NCAR	50	10	1	North Sea	NMC grid data
Sardie and Warner (1985)	PSU/NCAR	80	10	1	Atlantic, Pacific oceans	NMC grid data, manual analysis
Grønås, Foss and Lystad (1986, 1987)	NMI mesoscale	Nested grids, 150, 50 and 25	10	7	Norwegian Sea	ECMWF grid
Nørdeng (1987)	NMI mesoscale	50	10	2	Norwegian Sea	ECMWF grid

that can be taken to improve the observational base. Radar reflectivity data can be used to track the movement of storm centers and predict areas susceptible to high winds by charting the velocities of convective cells (Monk et al. 1987).

In view of the difficulty of obtaining high-resolution three-dimensional fields of the basic variables for insertion in numerical models, it is unlikely that the very fine-mesh limited-area models now under development will have a dramatic impact on polar-low prediction. While it is probable that they will result in better predictions of the larger size lows and will achieve some success in predicting smaller systems that are sparked by resolvable upper-level vorticity advections, it is unlikely that they will improve the prediction of the small seemingly random vortices that have been described elsewhere in this review. Clearly, the forecaster will continue to play a major role in polar-low prediction for the foreseeable future. The application of interpretive skills to buoy and ship data, satellite images, model-based analyses, and numerical forecasts offers the best route for advancing the monitoring and prediction of polar lows over the oceans.

## 9. Summary and conclusions

This review paper highlights the diversity of mesoscale phenomena that exist in polar air masses, and the forecasting problems that they entail. We have looked at polar lows from the standpoints of observation, theory, numerical modeling, and forecasting. From the observational standpoint it is clear that a variety of systems fall under the general heading of polar lows. We have organized the review of case studies on the basis of a combination of observational and physical considerations. This classification scheme is aimed more at diagnosing common types of developments rather than as a classification for its own sake. Further work in this direction is still needed to resolve issues such as whether the small, hurricane-like vortices seen in some cases should be regarded as a distinct type of polar low or as a substructure embedded within a larger, subsynoptic system.

It is clear that progress towards understanding and forecasting these varied phenomena depends on continued research efforts. If the subject is to advance, far more observations of the type taken during the Arctic Cyclone Experiment are urgently required. Since these maritime phenomena cannot be resolved with the current observational networks, they require special observations that can only be obtained by aircraft. Extensive field studies are needed to obtain multilevel observations during the life cycles of a representative sample of polar lows to resolve the many remaining questions regarding the triggering mechanisms and energetics of these fascinating and sometimes destructive storms.

Theoretical investigators in the past have tended to divide into two schools of thought, one school emphasizing baroclinic effects and the other championing CISK or other heating mechanisms. Lately there has been widespread recognition that the interaction of both mechanisms is important. Accordingly, the problem has become more complex, and it has become increasingly difficult to advance theoretical understanding using only simple models, though these still have a place. Particularly promising for future advancement are the regional primitive-equation models that are now under development at a number of research centers and that are coming into operational use at some forecast centers. These mesoscale models offer the opportunity for a wide variety of experimentation on the polar low problem.

Polar lows, with their rapid development and small scales, present a special challenge to the operational forecaster. The ability to forecast polar lows will benefit from advances on several fronts: improved observations (drifting buoys, coastal weather radars, satellite systems), the application of regional numerical weather prediction models with finer resolution to represent polar-low scale developments, continued refinement of empirical techniques, and further basic research.

*Acknowledgments.* The authors wish to thank Professor Erik Rasmussen and Dr. Melvin Shapiro for helpful conversations. The comments of anonymous reviewers were much appreciated. This material was

based upon work supported by the National Science Foundation under Grants ATM-8318857 and ATM-8421396-01. This review is based, in part, on a paper delivered at the seminar on the Nature and Prediction of Extratropical Weather Systems, 7–11 September 1987, sponsored by the European Centre for Medium Range Weather Forecasting (Reed 1987).

## REFERENCES

- Anderson, R. K., J. P. Ashman, F. Bittner, G. R. Farr, E. W. Ferguson, V. J. Oliver and A. H. Smith, 1969: Application of meteorological satellite data in analysis and forecasting. ESSA Tech. Rep. NES51, Government Printing Office, Washington, D.C. [NTIS AD-697033.]
- Billing, H., I. Haupt and W. Tonn, 1983: Evolution of a hurricane-like cyclone in the Mediterranean Sea. *Beitr. Phys. Atmos.*, **56**, 508–510.
- Blumen, W., 1980: On the evolution and interaction of short and long baroclinic waves of the Eady type. *J. Atmos. Sci.*, **37**, 1984–1993.
- Bratseth, A. M., 1985: A note on CISK in polar air masses. *Tellus*, **37A**, 403–406.
- Brown, R. A., 1980: Longitudinal instabilities and secondary flows in the Planetary boundary layer: A review. *Rev. Geophys. Space Phys.*, **18**, 683–697.
- Browning, K. A., and F. F. Hill, 1985: Mesoscale analysis of a polar trough interacting with a polar front. *Quart. J. Roy. Meteor. Soc.*, **111**, 445–462.
- Businger, S., 1985: The synoptic climatology of polar low outbreaks. *Tellus*, **37**, 419–432.
- , 1987: The synoptic climatology of polar low outbreaks over the Gulf of Alaska and Bering Sea. *Tellus*, **39**, 307–325.
- , and P. V. Hobbs, 1987: Mesoscale and synoptic scale structures of two comma cloud systems over the Pacific Ocean. *Mon. Wea. Rev.*, **115**, 1909–1928.
- , and B. Walter, 1988: Comma cloud development and associated rapid cyclogenesis over the Gulf of Alaska: a case study using aircraft and operational data. *Mon. Wea. Rev.*, **116**, 1103–1123.
- , and R. Reed, 1989: *Polar and Arctic Lows*. P. Twitchell, Ed., A. Deepak Publishing.
- Carlson, T., 1980: Airflow through midlatitude cyclones and the comma cloud pattern. *Mon. Wea. Rev.*, **108**, 1498–1509.
- Carleton, A. M., 1985: Satellite climatological aspects of the “polar low” and “instant occlusion.” *Tellus*, **37**, 433–450.
- Carr, F. H., and J. P. Millard, 1985: A composite study of comma clouds and their association with severe weather over the Great Plains. *Mon. Wea. Rev.*, **113**, 370–387.
- Charney, J. G., and A. Eliassen, 1964: On the growth of hurricane depression. *J. Atmos. Sci.*, **21**, 68–75.
- Duncan, C. N., 1977: A numerical investigation of polar lows. *Quart. J. Roy. Meteor. Soc.*, **103**, 255–268.
- , 1978: Baroclinic instability in a reversed shear flow. *Meteor. Mag.*, **107**, 17–23.
- Emanuel, K. A., 1986: An air–sea interaction theory for tropical cyclones. Part I: Steady-state maintenance. *J. Atmos. Sci.*, **43**, 585–604.
- , and R. Rotunno, 1989: Polar lows as Arctic hurricanes. *Tellus*, **41A**, 1–170.
- Ernst, J. A., and M. Matson, 1983: A Mediterranean tropical storm? *Weather*, **38**, 332–337.
- Forbes, G. S., and W. D. Lottes, 1985: Classification of mesoscale vortices in polar airstreams and the influence of the large-scale environment on their evolutions. *Tellus*, **37**, 132–155.
- Gall, R. L., 1976: The effects of latent heat release in growing baroclinic waves. *J. Atmos. Sci.*, **33**, 1686–1701.
- Grønås, S., A. Foss and M. Lystad, 1986a: Numerical simulations of polar lows in the Norwegian Sea. Part I: The model and simulations of the polar low 26–27 February 1984. Tech. Rept. No. 5, Norwegian Meteorological Institute, Oslo, 51 pp.
- , —, and —, 1986b: Numerical simulations of polar lows in the Norwegian Sea. Part II: Simulations of six synoptic situations. Tech. Rept. No. 18, Norwegian Meteorological Institute, Oslo, 32 pp.
- , —, and —, 1987: Numerical simulations of polar lows in the Norwegian Sea. *Tellus*, **39**, 334–353.
- Harley, D. G., 1960: Frontal contour analysis of a “polar low”. *Meteor. Mag.*, **89**, 146–147.
- Harrold, T. W., and K. A. Browning, 1969: The polar low as a baroclinic disturbance. *Quart. J. Roy. Meteor. Soc.*, **95**, 710–723.
- Kellogg, W. W., and P. F. Twitchell, 1986: Summary of the Workshop on Arctic Lows 9–10 May 1985, Boulder, Colorado. *Bull. Amer. Meteor. Soc.*, **67**, 186–193.
- Locatelli, J. D., P. V. Hobbs and J. A. Werth, 1982: Mesoscale structures of vortices in polar air streams. *Mon. Wea. Rev.*, **110**, 1417–1433.
- Lyll, I. T., 1972: The polar low over Britain. *Weather*, **27**, 378–390.
- Lystad, M., Ed., 1986: Polar lows in the Norwegian, Greenland and Barents Seas. Final Rep., Polar Lows Project. The Norwegian Meteorological Institute, Oslo, 196 pp.
- Mansfield, D. A., 1974: Polar Lows: The development of baroclinic disturbances in cold air outbreaks. *Quart. J. Roy. Meteor. Soc.*, **100**, 541–554.
- Mayengon, R., 1984: Warm core cyclones in the Mediterranean. *Mar. Wea. Log.*, **28**, 6–9.
- McGinnigle, J. B., M. V. Young and M. J. Bader, 1988: The development of instant occlusions in the north Atlantic. Met. 0.15 Internal Report, Meteorological Office, London Road, Bracknell, 25 pp.
- McMurdie, L. A., and K. B. Katsaros, 1985: Atmospheric water distribution in a midlatitude cyclone observed by the Seasat scanning multichannel microwave radiometer. *Mon. Wea. Rev.*, **113**, 584–598.
- Meteorological Office, 1962: *A Course in Elementary Meteorology*. Met. 0.707, Her Majesty's Stationary Office, London, WC1V 6HB, 189 pp.
- Midtbø, K. H., 1986: Polar low forecasting. *Proceedings of the International Conference on Polar Lows*, Oslo, The Norwegian Meteorological Institute, 363 pp.
- Monk, G. A., L. A. Browning and P. Konas, 1987: Forecasting applications of radar-derived precipitation echo velocities in the vicinity of polar lows. *Tellus*, **39**, 426–433.
- Monteverdi, J. P., 1976: The single air mass disturbance and precipitation characteristics at San Francisco. *Mon. Wea. Rev.*, **104**, 1289–1296.
- Mudrick, S. E., 1974: A numerical study of frontogenesis. *J. Atmos. Sci.*, **31**, 869–892.
- Mullen, S. L., 1979: An investigation of small synoptic-scale cyclones in polar air streams. *Mon. Wea. Rev.*, **107**, 1636–1647.
- , 1982: Cyclone development in the polar airstreams over the wintertime continent. *Mon. Wea. Rev.*, **110**, 1664–1676.
- , 1983: Explosive cyclogenesis associated with cyclones in polar air streams. *Mon. Wea. Rev.*, **111**, 1537–1553.
- Nordeng, T. E., 1987: The effect of vertical and slantwise convection on the simulation of polar lows. *Tellus*, **39**, 354–375.
- Økland, H., 1977: On the intensification of small-scale cyclones formed in very cold air masses heated over the ocean. Inst. Rep. Ser. No. 26, Institutt for Geofysikk, Universitet i Oslo, 25 pp.
- , 1987: Heating by organized convection as a source of polar low intensification. *Tellus*, **39**, 397–407.
- Ooyama, K., 1969: Numerical simulation of the life cycle of tropical cyclones. *J. Atmos. Sci.*, **26**, 3–40.
- Orlanski, I., 1986: Localized baroclinicity: a source for meso- $\alpha$  cyclones. *J. Atmos. Sci.*, **43**, 2857–2885.
- Parsons, D. B., and P. V. Hobbs, 1983: The mesoscale and microscale structure and organization of clouds and precipitation in mid-latitude cyclones. Part XI: Comparisons between observational and theoretical aspects of rainbands. *J. Atmos. Sci.*, **40**, 2377–2397.

- Pedgley, D. E., 1968: A meso-scale snow system. *Weather*, **23**, 469-476.
- Rabbe, A., 1987: A polar low over the Norwegian Sea, 29 February-1 March 1984. *Tellus*, **39**, 326-333.
- Rasmussen, E., 1977: The polar low as a CISK-phenomenon. Rep. No. 6, Inst. Teoret. Meteor., Kobenhavns Universitet, Copenhagen, 77 pp.
- , 1979: The polar low as an extratropical CISK disturbance. *Quart. J. Roy. Meteor. Soc.*, **105**, 531-549.
- , 1981: An investigation of a polar low with a spiral cloud structure. *J. Atmos. Sci.*, **38**, 1785-1792.
- , 1983: A review of meso-scale disturbances in cold air masses. *Mesoscale Meteorology-Theories, Observations and Models*, D. K. Lilly and T. Gal-chen, Eds., Reidel Publishing, 247-283.
- , 1985a: A case study of a polar low development over the Barents Sea. *Tellus*, **37A**, 407-418.
- , 1985b: A case study of a polar low development over the Barents Sea. Polar Lows Project Technical Rep. The Norwegian Meteorological Institute, Oslo, 42 pp.
- , 1985c: Paskestormen et baroklink polart lavryk. *Vejret*, **4-7 Argang**, 3-17.
- , and M. Lystad, 1987: The Norwegian polar lows project: a summary of the international conference on polar lows. *Bull. Amer. Meteor. Soc.*, **68**, 801-816.
- , and C. Zick, 1987: A subsynoptic vortex over the Mediterranean Sea with some resemblance to polar lows. *Tellus*, **39**, 408-425.
- Reed, R. J., 1979: Cyclogenesis in polar air streams. *Mon. Wea. Rev.*, **107**, 38-52.
- , 1987: Polar lows. *Seminar on the Nature of Prediction of Extratropical Weather Systems*, 213-236. [Available from ECMWF, Shinfield Park, Reading, RG2 9AX, U.K.]
- , and W. Blier, 1986a: A case study of comma cloud development in the Eastern Pacific. *Mon. Wea. Rev.*, **114**, 1681-1695.
- , and —, 1986b: A further case study of comma cloud development in the Eastern Pacific. *Mon. Wea. Rev.*, **114**, 1696-1708.
- , and C. N. Duncan, 1987: Baroclinic instability as a mechanism for the serial development of polar lows: A case study. *Tellus*, **39**, 376-384.
- Rosenthal, S. L., 1971: The response of a tropical cyclone model to variations in boundary layer parameters, initial conditions, lateral boundary conditions, and domain size. *Mon. Wea. Rev.*, **99**, 767-777.
- Sardie, J. M., and T. T. Warner, 1983: On the mechanism for the development of polar lows. *J. Atmos. Sci.*, **40**, 869-881.
- , and —, 1985: A numerical study of the development mechanisms of polar lows. *Tellus*, **37**, 460-477.
- Seaman, N. L., 1983: Simulation of a mesoscale polar low in the North Sea. *Sixth Conference on Numerical Weather Prediction*. Boston, Amer. Meteor. Soc., 24-30.
- , H. Otten and R. A. Anthes, 1982: A rapidly developing polar low in the North Sea of January 2, 1979. *First International Conference on Meteorology and Air/Sea Interaction of the Coastal Zone*, the Hague, Netherlands.
- Shapiro, M. A., and L. S. Fedor, 1986: The Arctic cyclone expedition, 1984: Research and aircraft observations of fronts and polar lows over the Norwegian and Barents Sea, Part 1. Polar Lows Project, Technical Rep. No. 20, The Norwegian Meteorological Institute, Oslo, 56 pp.
- , L. S. Fedor and T. Hampel, 1987: Research aircraft measurements within a polar low over the Norwegian Sea. *Tellus*, **37**, 272-306.
- Staley, D. O., and R. L. Gall, 1977: On the wavelength of maximum baroclinic instability. *J. Atmos. Sci.*, **34**, 1679-1688.
- Sutcliffe, R. C., and A. G. Forsdyke, 1950: The theory and use of upper air thickness patterns in forecasting. *Quart. J. Roy. Meteor. Soc.*, **76**, 189-217.
- Uccellini, L. W., and P. J. Kocin, 1987: The interaction of jet streak circulations during heavy snow events along the east coast of the United States. *Weather Forecasting*, **1**, 289-308.
- Wallace, J. M., and P. V. Hobbs, 1977: *Atmospheric Science: an Introductory Survey*. Academic Press, 417 pp.
- World Meteorological Organization, 1973: The Use of Satellite Pictures in Weather Analysis and Forecasting. Technical Note. No. 124, WMO No. 333. 275 pp. [Available from the Secretariat of the World Meteorological Organization, Geneva, Switzerland.]
- Zick, C., 1983: Method and results of an analysis of comma cloud developments by means of vorticity fields from upper tropospheric satellite wind data. *Meteorol. Rdsch.*, **36**, 69-84.
- , 1986: Two Meteosat film scenes showing polar lows over the Norwegian Sea. *Proceedings of the International Conference on Polar Lows*, Oslo, The Norwegian Meteorological Institute, 363 pp.